


Downregulation of *HbFPS1* affects rubber biosynthesis of *Hevea brasiliensis* suffering from tapping panel dryness

Zhiyi Nie^{1,2} , Guijuan Kang^{1,2}, Dong Yan¹, Huaide Qin^{1,2}, Lifu Yang³ and Rizhong Zeng^{1,2,*}

¹Rubber Research Institute & Key Laboratory of Biology and Genetic Resources of Rubber trees, Ministry of Agriculture and Rural Affairs of the People's Republic of China, Chinese Academy of Tropical Agricultural Sciences, Haikou 571101, Hainan, China,

²Key Laboratory of Materials Engineering for High Performance Natural Rubber, Hainan Province, Chinese Academy of Tropical Agricultural Sciences, Haikou 571101, Hainan, China, and

³Institute of Scientific and Technical Information, Chinese Academy of Tropical Agricultural Sciences, Haikou 571101, Hainan, China

Received 3 August 2022; revised 1 November 2022; accepted 9 December 2022; published online 16 December 2022.

*For correspondence (e-mail hnrz@aliyun.com).

SUMMARY

Tapping panel dryness (TPD) is a century-old problem that has plagued the natural rubber production of *Hevea brasiliensis*. TPD may result from self-protective mechanisms of *H. brasiliensis* in response to stresses such as excessive hormone stimulation and mechanical wounding (bark tapping). It has been hypothesized that TPD impairs rubber biosynthesis; however, the underlying mechanisms remain poorly understood. In the present study, we firstly verified that TPD-affected rubber trees exhibited lower rubber biosynthesis activity and greater rubber molecular weight compared to healthy rubber trees. We then demonstrated that *HbFPS1*, a key gene of rubber biosynthesis, and its expression products were downregulated in the latex of TPD-affected rubber trees, as revealed by transcriptome sequencing and iTRAQ-based proteome analysis. We further discovered that the farnesyl diphosphate synthase HbFPS1 could be recruited to small rubber particles by HbSRPP1 through protein–protein interactions to catalyze farnesyl diphosphate (FPP) synthesis and facilitate rubber biosynthesis initiation. FPP content in the latex of TPD-affected rubber trees was significantly decreased with the downregulation of HbFPS1, ultimately resulting in abnormal development of rubber particles, decreased rubber biosynthesis activity, and increased rubber molecular weight. Upstream regulator assays indicated that a novel regulator, MYB2-like, may be an important regulator of downregulation of *HbFPS1* in the latex of TPD-affected rubber trees. Our findings not only provide new directions for studying the molecular events involved in rubber biosynthesis and TPD syndrome and contribute to rubber management strategies, but also broaden our knowledge of plant isoprenoid metabolism and its regulatory networks.

Keywords: *Hevea brasiliensis*, rubber biosynthesis, farnesyl diphosphate synthase, tapping panel dryness, transcriptome sequencing, iTRAQ, protein–protein interaction, MYB transcription factor.

INTRODUCTION

Tapping panel dryness (TPD) is a syndrome that affects rubber trees (*Hevea brasiliensis* Muell. Arg.), the only economically viable source of natural rubber (NR), which is an important raw industrial material used in various economic sectors worldwide. TPD may be a self-protective mechanism of rubber trees in response to excessive stimulation with ethylene (ET) and bark tapping during rubber production (Peng et al., 2011). The first TPD symptom is the appearance of partial dry zones along the tapping panel of the tree bark. These eventually become completely dry

zones, and finally, there is a complete lack of latex flow upon tapping (Sookmark et al., 2002) (Figure S1). TPD has been jeopardizing rubber production for over 100 years. It is a critical factor affecting NR yield in rubber plantations, causing 10–40% NR yield losses annually in one rubber tree cultivation cycle (Gebelin et al., 2013). The underlying mechanisms of TPD onset have been extensively investigated, with accumulating information indicating that it is a complex physiological disorder (Chen et al., 2003; d'Auzac & Jacob, 1989; de Faÿ & Jacob, 1989). TPD can be detected early by monitoring latex peroxidase activity and the

inorganic phosphate (Pi) content (Tristama et al., 2019). There is evidence that TPD susceptibility is an intrinsic genetically inherited characteristic (Jacob, 1989; Yang & Fan, 1995) that can be induced by overexploitation, i.e., excessive tapping and/or ET overstimulation (Chrestin, 1989; Fan & Yang, 1984; Faridah et al., 1996; Li et al., 2020; Nie et al., 2016). Nevertheless, the TPD-associated molecular mechanisms are still rather elusive. Thus, they should be elucidated entirely to accelerate the development of techniques for controlling this disorder.

Cytological and physiological studies have revealed that rubber tree TPD might result from programmed cell death (PCD) activation, triggered by various stress responses, to protect the tree and enhance survival (Chen et al., 2003; de Faÿ, 2011; Li et al., 2016; Peng et al., 2011; Venkatachalam et al., 2009). In TPD-affected rubber trees, potential PCD pathway-related genes are induced. On the other hand, several rubber biosynthesis-related key genes, such as rubber elongation factor (*REF*), *HbTOM20*, small rubber particle protein (*SRPP*), and mevalonate-5-phosphate kinase (*PMK*), are downregulated (Li et al., 2010, 2016; Liu et al., 2015). Notably, two PCD-associated proteins, *HbTCTP* and *HbMC1*, were found to interact with *REF* (Deng et al., 2016; Liu et al., 2019). These studies demonstrated that rubber biosynthesis occurring on the rubber particles (RPs) in the laticifers might be greatly affected by TPD, resulting in significantly reduced rubber production.

Although many previous investigations have been conducted on the mechanisms underlying TPD (Chen et al., 2003; de Faÿ, 2011; Li et al., 2010, 2016; Venkatachalam et al., 2009), it remains uncertain whether TPD affects rubber biosynthesis of the laticiferous cells. The efficiency of rubber biosynthesis by laticiferous cells is one of the three major factors determining rubber production (Yamaguchi et al., 2020). Rubber is a biopolymer synthesized in laticiferous cells by rubber transferase (*cis*-prenyltransferase [*CPT*], EC 2.5.1.20) together with related proteins such as *REF* and *SRPP* (Men et al., 2019). Two substrates are essential for rubber biosynthesis. The first is the precursor isopentenyl pyrophosphate (IPP) from sucrose hydrolysis via the cytosolic mevalonate (MVA) pathway or the plastidic 2-C-methyl-D-erythritol-4-phosphate (MEP) pathway (Chow et al., 2012). The second is the allylic pyrophosphate (APP) initiator such as farnesyl diphosphate (FPP), geranyl pyrophosphate (GPP), or geranylgeranyl pyrophosphate (GGPP) (Cornish, 2001), among which FPP synthesized by farnesyl diphosphate synthase (FPS) is the most efficient (Xie et al., 2008). A recent investigation revealed that laticiferous cells have a higher proportion of miRNA- and *trans*-acting siRNA-mediated transcript cleavage activity than other tissues, and several important biological pathways such as hormonal signaling and rubber biosynthesis are affected by post-transcriptional silencing in laticiferous cells (Leclercq et al., 2020). Therefore, latex, the cytoplasm of

laticifers (Hagel et al., 2008), is a more suitable material for studying the effects of TPD on rubber biosynthesis than the bark tissue used previously (Li et al., 2016; Liu et al., 2015). Moreover, a combined analysis of the latex transcriptome and proteome to identify variation before and after TPD could more accurately elucidate the impact of TPD on laticiferous cells, especially on the molecular mechanisms of rubber biosynthesis, than a transcript-level analysis alone.

The present study reports the physiological parameters, rubber biosynthesis activity, average rubber molecular weight, and latex transcriptome and proteome in healthy and TPD-affected rubber trees. We focused on the expression of rubber biosynthesis-related genes and proteins, and found that the level of FPP synthase *HbFPS1*, a critical rate-limiting enzyme in the pathway of rubber biosynthesis (Cornish, 1993; Men et al., 2019), was significantly altered. *HbFPS1* expression regulation and its subcellular relocation through protein–protein interactions were further elucidated. These results indicate that *HbFPS1* down regulation is the primary determinant for the reduction of rubber biosynthesis activity and the increase of rubber molecular weight in TPD-affected rubber trees.

RESULTS

Latex physiological parameters of healthy and TPD-affected trees

Rubber yield and physiological parameters were measured to analyze latex metabolism in rubber trees during different stages of TPD. Significant decreases in NR yield, Pi content, and thiol (RSH) content were observed (Figure 1a,c,e), while remarkable increases in sucrose content and rubber molecular weight were observed in latex sample T4 (Figure 1b,j). No significant changes in Mg²⁺ content were observed in latex samples T2 and T4 (Figure 1d). These results indicate that the latex metabolic activity and reactive oxygen species (ROS) scavenging ability decrease as the TPD symptoms worsen.

Rubber biosynthesis activity in latex from healthy and TPD-affected trees

It has been hypothesized that TPD influences rubber biosynthesis through changing the expression of rubber biosynthesis-related genes in the latex or bark (Li et al., 2010, 2016; Liu et al., 2015). We monitored the rubber biosynthesis activity of latex from healthy and TPD-affected trees by *in vitro* rubber biosynthesis efficiency assays (Figure 1i). Rubber biosynthesis activity was decreased significantly in T4 compared to H (healthy trees), suggesting that rubber yield might be directly reduced in TPD-affected trees. Furthermore, although the average RP size and the abundance of large RPs (LRPs) with a volume mean diameter (VMD) of more than 1.0 µm were not significantly different in TPD-affected trees compared to

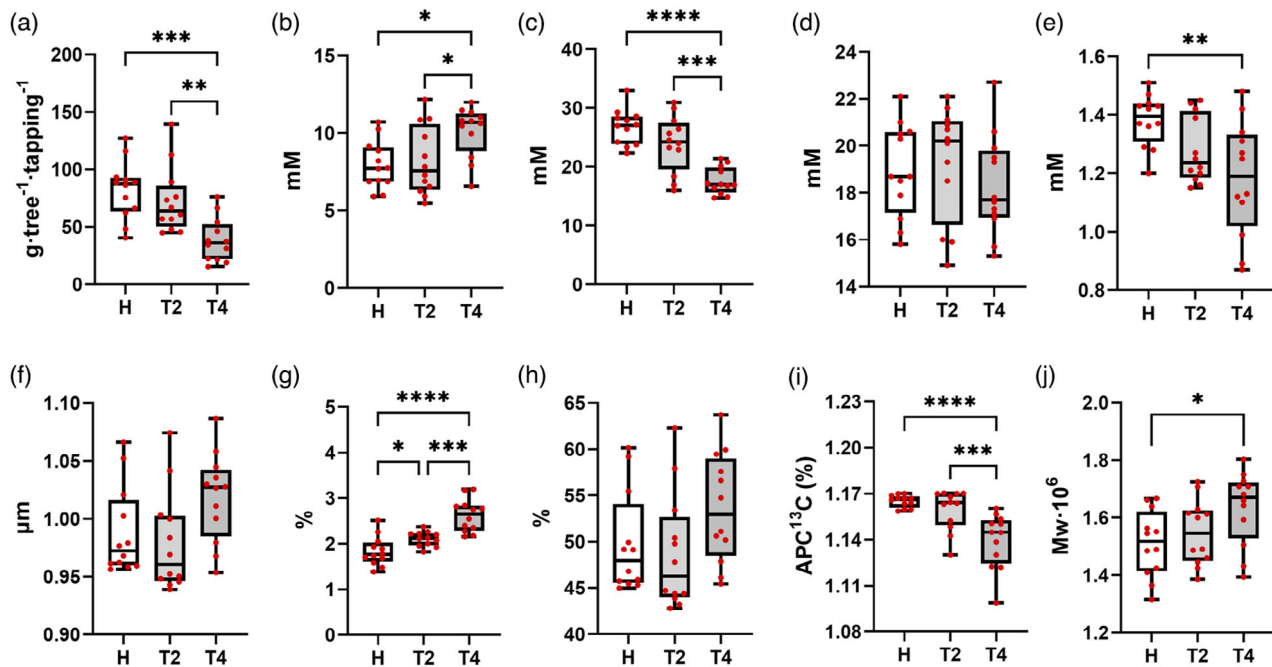


Figure 1. Latex yield and physiological parameters of healthy and TPD-affected rubber trees. (a) Latex yield. (b) Sucrose content. (c) Pi content. (d) Mg^{2+} content. (e) RSH content. (f) Average RP size. (g) Percentage of SRPs (VMD < $0.3 \mu m$). (h) Percentage of LRPs (VMD > $1.0 \mu m$). (i) Rubber biosynthesis activity of latex. (j) Rubber average molecular weight. One-way analysis of variance and the Student–Newman–Keuls test were performed to identify significant differences between groups. * $P < 0.05$, ** $P < 0.01$, *** $P < 0.001$, **** $P < 0.0001$, $n = 12$. TPD, tapping panel dryness; RP, rubber particle; SRPs, small rubber particles; LRPs, large rubber particles; VMD, volume mean diameter; APC^{13C} , atom percentage of ^{13}C .

healthy trees (Figure 1f,h), the abundance of small RPs (SRPs) with a VMD of less than $0.3 \mu m$ was significantly higher in TPD-affected trees than in healthy trees (Figure 1g). This indicates that the RPs of TPD-affected trees may undergo abnormal development due to reduction in rubber biosynthesis. Notably, Mg^{2+} content in the latex C-serum is correlated with rubber biosynthesis activity (Scott et al., 2003). However, in the present study, no significant differences were observed in the Mg^{2+} content of the latex C-serum between TPD-affected trees and healthy trees, despite significantly decreased rubber biosynthesis activity. This may be due to the instability of the lutoids in TPD latex, which are prone to rupture and release of Mg^{2+} , resulting in inaccurate C-serum Mg^{2+} content determination results. Herlinawati et al. (2022) advocated that the Mg^{2+} measurements in TPD latex have relatively poor reproducibility and are susceptible to seasonal effects. Therefore, these results may not be a true reflection of the Mg^{2+} content in the C-serum.

Identification of differentially expressed genes using transcriptome sequencing

In total, 369 600 064 high-quality reads were obtained from the H, T2, and T4 cDNA libraries. Of these, 325 260 983 reads were mapped to the *H. brasiliensis* reference genome. In total, 29 004 unique genes were detected in the latex of healthy and TPD-affected trees (additional information in

Table S1). The T2 group exhibited 66 (47 upregulated and 19 downregulated) and the T4 group exhibited 2312 (1178 upregulated and 1134 downregulated) differentially expressed genes (DEGs) compared with the H group, respectively (Table S2). Thus, there were significant differences in the gene expression profiles in the latex of healthy and TPD-affected trees. These differences were more profound between healthy trees and the T4 TPD-affected rubber trees.

Identification of differentially abundant proteins by iTRAQ technology

In total, 58 309 spectra, 17 971 peptides, and 3357 proteins were identified from 535 879 total spectra, with a false discovery rate (FDR) of $\leq 1\%$. The T2 group exhibited 168 (85 upregulated and 83 downregulated) and the T4 group exhibited 171 (70 upregulated and 101 downregulated) differentially abundant proteins (DAPs) compared with the H group, respectively, with a fold change value of >1.2 or <0.85 and $P < 0.05$ (Table S3).

Comparative analysis of DEGs and DAPs

To evaluate the relationship between transcript levels and protein abundance, we compared the identified DAPs and DEGs. In the T2_H (T2 group compared with the H group) and T4_H (T4 group compared with the H group) comparisons, 48 shared DEGs and 67 shared DAPs were identified (Figure S2a). Specifically, 11 DEGs and 24 DAPs were

upregulated and 37 DEGs and 43 DAPs were downregulated in both comparisons. Furthermore, in T2_H and T4_H, 1 and 19 DAPs and their corresponding DEGs were identified, respectively (Figure S2a). No DAPs were co-regulated with their corresponding DEGs in T2_H, while 12 co-regulated DAPs (eight with increased and four with decreased abundance) were identified in T4_H (Figure S2b). Finally, Pearson correlation analysis between DAPs and DEGs indicated that in T4_H, protein abundance changes were significantly correlated with changes in their corresponding transcript levels ($P > 0.05$ in T2_H and $P < 0.01$ in T4_H). However, the correlation was very low ($r = 0.024$ in T2_H and $r = 0.104$ in T4_H) (Figure S2c–e).

KEGG pathway annotations of DAPs and DEGs

The 2330 DEGs and 272 DAPs identified above were classified into different KEGG pathways. In the T2_H comparison, 168 DAPs were classified into 52 pathways, while 66 DEGs were classified into 14 pathways (Figure 2a). Furthermore, 11 and two KEGG pathways were significantly overrepresented ($P \leq 0.05$) in T2_H DAPs and DEGs, respectively (Figure 2c; Table S4). In the T4_H comparison, 171 DAPs were classified into 50 pathways, while 2312 DEGs were classified into 139 pathways (Figure 2b). Eight and 12 KEGG pathways were significantly overrepresented in T4_H DAPs and T4_H DEGs, respectively (Figure 2c; Table S4). These 2330 DEGs were significantly enriched in 14 KEGG pathways mainly related to energy metabolism (ko00190, ko00195, ko00920), carbohydrate metabolism (ko00020, ko00562, ko00620), PCD (ko03050), and signal transduction/information processing (ko03008, ko03020, ko03040, ko03050, ko04075). The 272 DAPs were significantly enriched in 16 KEGG pathways related to energy metabolism (ko00010, ko00710, ko01200), lipid metabolism (ko00062, ko00564, ko00565, ko00590), carbohydrate metabolism (ko00010, ko00020, ko01200), nucleotide/amino acid metabolism (ko00240, ko00270, ko00350, ko00460), ROS scavenging (ko00270, ko00480), PCD (ko03050, ko04141), and signal transduction/information processing (ko03050, ko04141, ko04144) (Figure 2c; Table S4).

DEGs and DAPs involved in rubber biosynthesis

In the pre-IPP steps of the rubber biosynthesis pathway, the IPP monomer is mainly synthesized from the MVA pathway (Sando et al., 2008; Men et al., 2019). We identified two DAPs and one DEG encoding an enzyme involved in the MVA pathway. Specifically, a 3-hydroxy-3-methylglutaryl-CoA synthase (HMGS) was upregulated in both T2_H and T4_H, an acetyl-CoA C-acetyltransferase (ACAT) was downregulated in T4_H, and a DEG encoding a 3-hydroxy-3-methylglutaryl-CoA reductase (HMGR) was upregulated in T4_H. Besides the MVA pathway, the IPP monomer, used in rubber biosynthesis, may be produced by the MEP pathway (Chow et al., 2012). We identified a

DEG encoding a 1-deoxy-D-xylulose 5-phosphate synthase (DXS) involved in the MEP pathway that was downregulated in T4_H (Figure 2d; Tables S5 and S6). In addition, four DEGs and eight DAPs identified are linked to rubber biosynthesis. In the post-IPP steps of the rubber biosynthesis pathway, an oligomeric APP initiator (such as dimethylallyl pyrophosphate [DMAPP], GPP, FPP, or GGPP) is necessary for NR chain synthesis initiation. In the present study, a DAP and a DEG encoding an FPP synthase (*HbFPS1*, gene ID: scaffold0157_1428529, NCBI Reference Sequence: XM_021816653.1) were downregulated in both T2_H and T4_H and in T4_H, respectively. Moreover, a DEG encoding a GGPP synthase (GGPS) was upregulated in T4_H. It has been established that CPT and REF/SRPP family proteins play a significant role in rubber biosynthesis (Brown et al., 2017; Cornish, 2001; Dai et al., 2013; Epping et al., 2015; Yamashita et al., 2016). Accordingly, we identified two DEGs encoding CPT and REF/SRPP family proteins that were downregulated in T4_H, and one, two, and five REF/SRPP family DAPs that were upregulated in T2_H, T4_H, and both T2_H and T4_H, respectively (Figure 2d; Tables S5 and S6). The NR yield and rubber biosynthesis activity were significantly lower in TPD-affected trees than in healthy trees, which might result from downregulation of rubber biosynthesis-related genes or gene expression products. Among these, three rubber biosynthesis-related DEGs, encoding DSX, FPS (*HbFPS1*), and CPT, and two DAPs (ATAC and *HbFPS1*) were downregulated. Only the protein abundance of *HbFPS1* was significantly reduced during the early TPD stages (T2) and was further greatly diminished as TPD progressed (T4) (Figure 3b; Table S6), indicating that *HbFPS1* may be closely associated with TPD onset and progression.

Validation of gene expression by RT-qPCR

Among the 30 genes selected for validation (Table S7), 13 genes exhibited similar expression patterns ($P < 0.05$) between the RNA sequencing (RNA-seq) and real-time quantitative PCR (RT-qPCR) analyses, five genes exhibited similar expression patterns between the iTRAQ-based proteome and RT-qPCR analysis, and 11 genes exhibited similar expression patterns in all three analyses (Figure S3). A significant correlation was observed between the RNA-seq and RT-qPCR data when assessing the fold change values of the 30 selected genes ($r = 0.406$, $P < 0.01$). These results indicate that transcriptome sequencing is an accurate and efficient method for assessing gene expression in rubber tree latex.

FPS and FPP quantification in the latex of healthy and TPD-affected trees

DEG and DAP analyses indicated that *HbFPS1* and its corresponding protein were downregulated in the latex of TPD-affected trees (Figure 3a,b; Tables S5 and S6).

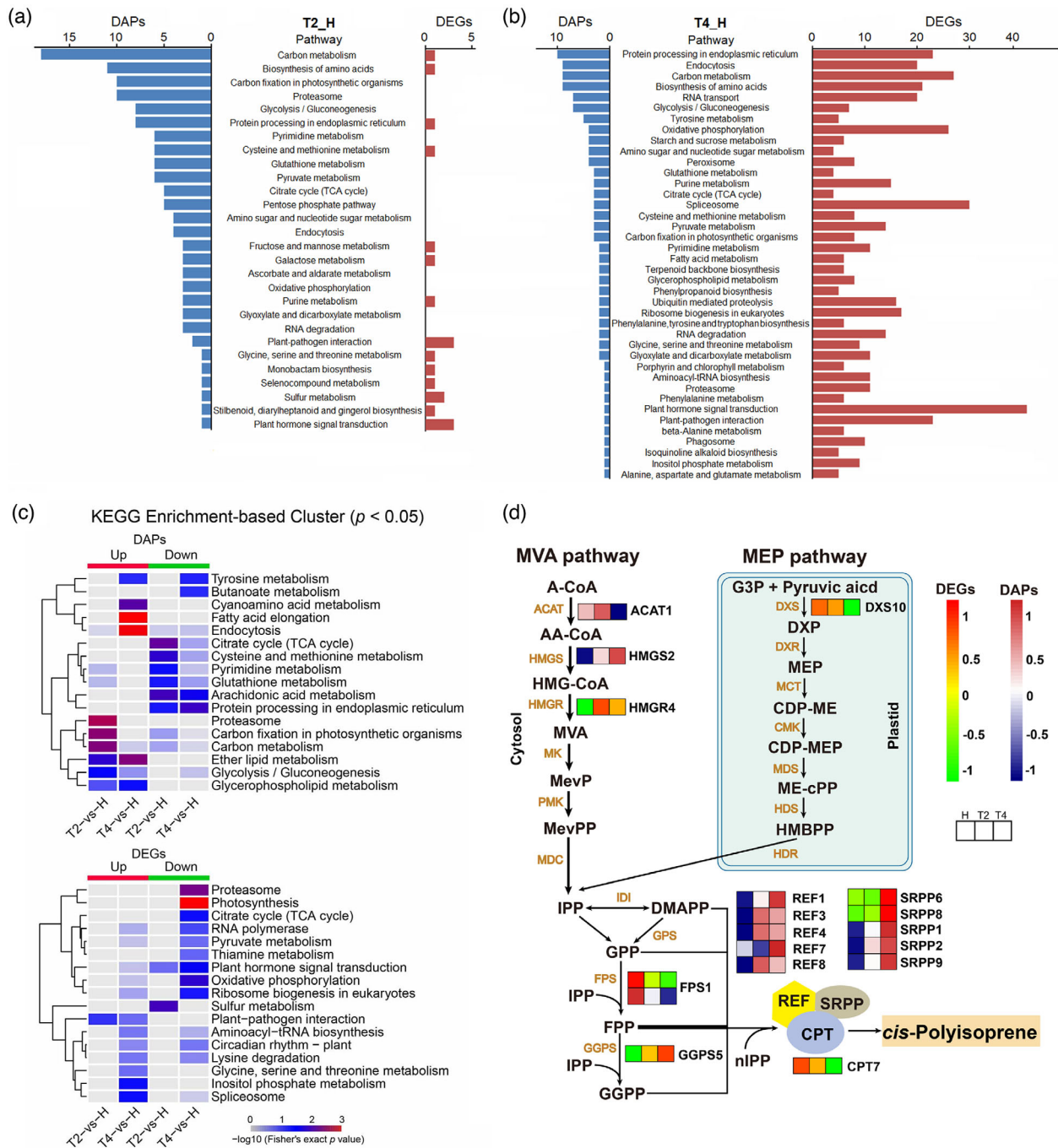


Figure 2. KEGG pathway analysis of DAPs and DEGs and expression profiles of rubber biosynthesis-related DAPs and DEGs. KEGG pathway annotations for DAPs and DEGs in comparisons of (a) T2_H and (b) T4_H. The numbers of DAPs (left) and DEGs (right) associated with a pathway are indicated. (c) KEGG enrichment-based cluster analysis of DAPs and DEGs ($P < 0.05$). (d) Expression profiles of DAPs and DEGs involved in rubber biosynthesis. DAPs, differentially abundant proteins; DEGs, differentially expressed genes; MVA, mevalonate; A-CoA, acetyl-CoA; ACAT, acetyl-CoA C-acetyltransferase; AA-CoA, acetoacetyl-CoA; HMGS, HMG-CoA synthase; HMG-CoA, 3-hydroxy-3-methyl-glutaryl-CoA; HMGR, HMG-CoA reductase; MK, mevalonate kinase; PMK, mevalonate-5-phosphate; MDC, mevalonate-5-pyrophosphate decarboxylase; G3P, glyceraldehyde-3-phosphate; DXS, DXP synthase; DXP, 1-deoxy-D-xylulose-5-phosphate; DXR, DXP reductoisomerase; MEP, 2-C-methyl-D-erythritol-4-phosphate; MCT, CDP-ME synthase; CDP-ME, 4-(cytidine-5'-diphospho)-2-C-methyl-D-erythritol; CMK, CDP-ME kinase; CDP-MEP, 2-phospho-4-(cytidine-5'-diphospho)-2-C-methyl-D-erythritol; MDS, ME-cPP synthase; ME-cPP, 2-C-methyl-D-erythritol-2,4-cyclodiphosphate; HDS, HMBPP synthase; HMBPP, 4-hydroxy-3-methylbut-2-enyl diphosphate; HDR, HMBPP reductase; IPP, isopentenyl pyrophosphate; IDI, IPP isomerase; DMAPP, dimethylallyl pyrophosphate; GPS, geranyl pyrophosphate synthase; GPP, geranyl pyrophosphate; FPS, farnesyl pyrophosphate synthase; FPP, farnesyl pyrophosphate; GGPS5, GGPP synthase; GGPP, geranylgeranyl pyrophosphate; CPT, *cis*-prenyltransferase; REF, rubber elongation factor; SRPP, small rubber particle protein.

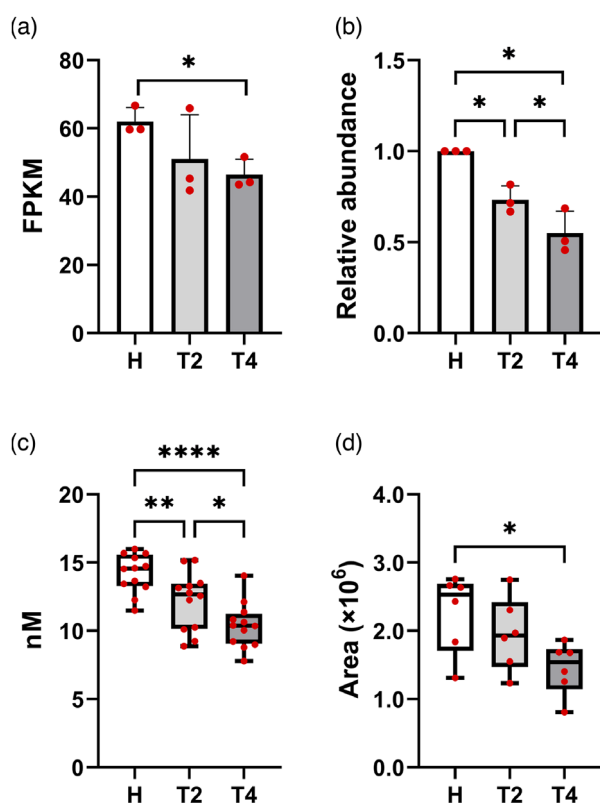


Figure 3. Relative gene expression and protein abundance of HbFPS1, FPS content, and relative FPP content in the latex of healthy and TPD-affected trees. (a) Relative gene expression of *HbFPS1*. (b) Relative protein abundance of HbFPS1. Data were derived from the RNA-seq transcriptome data FPKM values (*FDR < 0.05, $n = 3$) and the fold change values from the iTRAQ-based proteome data (Student's *t*-test, * $P < 0.05$, $n = 3$), respectively. (c) FPS content and (d) relative FPP content. One-way analysis of variance and the Student–Newman–Keuls test were performed to identify significant differences between groups. * $P < 0.05$, ** $P < 0.01$, **** $P < 0.0001$, $n = 6–12$. FPS, farnesyl pyrophosphate synthase; FPP, farnesyl pyrophosphate; TPD, tapping panel dryness.

Furthermore, a significant reduction in FPS content and its catalytic product FPP was detected in T2 and T4 and T4, respectively, by ELISA and GC-MS analysis, consistent with *HbFPS1* expression and its corresponding protein abundance (Figure 3c,d). Therefore, HbFPS1 may be directly involved in TPD development by affecting rubber biosynthesis in latex.

Effects of FPS and FPP contents on rubber biosynthesis

HbFPS1 was expressed in *Escherichia coli* BL21 (DE3) and purified (Figure S4a–c). The effects of FPS and FPP content on rubber biosynthesis were evaluated using an *in vitro* assay. The addition of FPP to the *in vitro* rubber biosynthesis system enhanced the rate of rubber biosynthesis. In contrast, rubber biosynthesis was inhibited in the assay without FPP (Figure 4a,b). When purified HbFPS1 was added, the rubber synthesis activity of the *in vitro* system

with latex as cofactor increased (Figure 4b). However, no significant change in rubber synthesis activity was found with washed RPs (WRPs) as cofactor (Figure 4a). This may be due to the FPS catalytic substrate GPP in the latex, which was absent in the WRPs. On the other hand, when alendronate sodium (an FPS inhibitor) was added to the system with latex as cofactor, the rubber biosynthesis activity showed a very significant reduction (Figure 4b). These results suggest that the decrease in FPP content due to the reduced HbFPS1 abundance in TPD-affected tree latex may be one of the critical reasons for the reduction in rubber biosynthesis activity in TPD-affected tree latex.

Moreover, a significant increase in rubber molecular weight was detected in the latex of T4, which reveals that TPD may influence the molecular weight of rubber. Increasing FPP or GPP concentrations decrease the molecular weight of synthesized rubber in the *in vitro* rubber biosynthesis system that uses WRPs as cofactor (Cornish, 2001). We analyzed the molecular weight of NR, which was synthesized by the *in vitro* rubber biosynthesis system with different FPP or FPS concentrations. The results show that the molecular weight of the synthesized rubber decreased with increasing FPP concentrations regardless of whether latex or WRPs were used as cofactor in the assay system (Figure 4c,d). In contrast, the addition of alendronate sodium to the assay using latex as cofactor significantly increased the molecular weight of synthesized rubber (Figure 4d). These results indicate that the increase in the molecular weight of rubber from TPD-affected trees might be caused by the decrease in the FPP content of the latex due to the decrease in the abundance of HbFPS1.

Differences in rubber biosynthesis activity, FPS, and HbSRPP1 abundance of RPs with different particle sizes

RP1 (having the smallest average particle size) exhibited the highest rubber biosynthesis activity, based on the *in vitro* assay, and this activity decreased significantly with the increase of RP size. No significant differences were observed in rubber biosynthesis activity among RP4 and RP5 and the control (Figure 5a). Correspondingly, HbSRPP1 had the highest abundance in RP1 and decreased with the increase of RP size (Figure 5c,d), while FPS was mainly present in RP1 (Figure 5b).

Relationship between HbSRPP1 and HbFPS1

RPs originate from the membrane of endoplasmic reticulum (ER) (Brown et al., 2017). We performed subcellular localization experiments of HbFPS1 and HbSRPP1 using *Nicotiana benthamiana* leaf epidermal cells. The fluorescence signal of the GFP-fused HbSRPP1 almost overlapped with that of OsSPP1-red fluorescent protein (RFP) (ER marker), indicating that HbSRPP1 is predominantly localized in the ER (Figure 6a–c). These results are in agreement with previously described localizations for HbSRPP1 (Brown

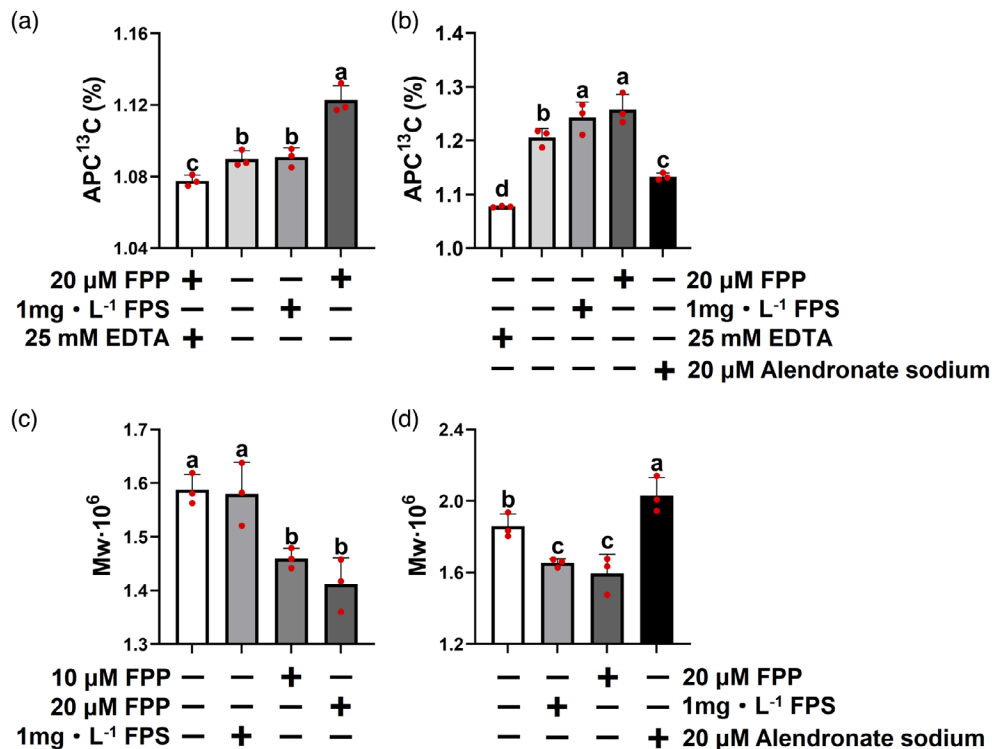


Figure 4. Effects of FPS and FPP concentrations on rubber biosynthesis efficiency and molecular weight *in vitro*. The effects of FPS and FPP concentrations on rubber biosynthesis efficiency and molecular weight were assessed using WRPs as cofactor in (a) and (c) and latex as cofactor in (b) and (d). The symbols + and - indicate differences in reaction buffer components. Data are presented as means \pm SE. One-way analysis of variance and the Student–Newman–Keuls test were performed to identify significant differences between groups. Different letters indicate significant differences ($P < 0.05$, $n = 3$). FPS, farnesyl pyrophosphate; FPP, farnesyl pyrophosphate; WRPs, washed rubber particles; APC¹³C, atom percentage of ¹³C.

et al., 2017). On the other hand, the fluorescence signal of GFP-fused HbFPS1 was detected in the space surrounding the chloroplasts (Figure 6g–i) and in the nucleoplasm (Figure 6j–l), suggesting that HbFPS1 is a soluble protein localized in the cytosol. These results are in agreement with a previous study of HbFPS1 (Adiwilaga & Kush, 1996; Cornish, 1993; Xie et al., 2008). In addition, HbFPS1 was not predicted to carry a signal peptide or contain any transmembrane domains according to the SignalP 4.1 and TMHMM 2.0 prediction algorithms, so it could also be detected in the ER (Figure 6d–f).

We further evaluated the relationship between HbSRPP1 and HbFPS1 and whether HbFPS1 is localized on RPs through protein–protein interactions with HbSRPP1. Co-expression assays of HbSRPP1 and HbFPS1 showed that co-localized fluorescence signals on the ER and the nuclear envelope could be visualized when HbSRPP1-RFP and HbFPS1-GFP constructs were co-infiltrated into *N. benthamiana* leaves (Figure 7a). We therefore performed individual yeast two-hybrid (Y2H) and bimolecular fluorescence complementation (BiFC) assays to identify potential protein–protein interactions among HbREF1, HbSRPP1 and HbFPS1. Individual Y2H assays showed that HbFPS1 interacts with HbSRPP1 (Figure 7b), and BiFC assays further indicated that their

interaction occurs on the intracellular membranes (Figure 7c). These observations undoubtedly confirm that HbFPS1 is relocated on RPs through the protein–protein interactions with HbSRPP1. Based on the results, we suggest a model for RP biogenesis and protein–protein interacting pattern among the rubber biosynthesis-related proteins (Figure 7d).

Y1H, EMSA, and Dual-LUC assays

In total, 29 positive colonies were obtained and sequenced by screening the latex cDNA library using triple dropout (TDO) plates (SD/–His–Leu–Trp) supplemented with 80 mM 3-amino-1,2,4-triazole (3-AT). Two candidates encoding transcription factors were obtained, namely, *HbEREBP1* (gene ID: scaffold0620_551771, NCBI Reference Sequence: HQ171930.1) and *MYB2-like* (gene ID: scaffold2277_3347, NCBI Reference Sequence: XM_021805772.1). The individual yeast one-hybrid (Y1H) assays showed that the cells with pGADT7-MYB2like/pHis-pHbFPS1 could grow on TDO plates with 80 or 120 mM 3-AT, whereas the cells with pGADT7-HbEREBP1/pHis-pHbFPS1 could grow on TDO plates with 80, 120, or 160 mM 3-AT (Figure 8a). The DNA–protein binding signal was detected for the recombinant HbEREBP1 and MYB2-like protein incubated with the *HbFPS1* promoter (Figure 8c), further confirming their binding to the *HbFPS1*

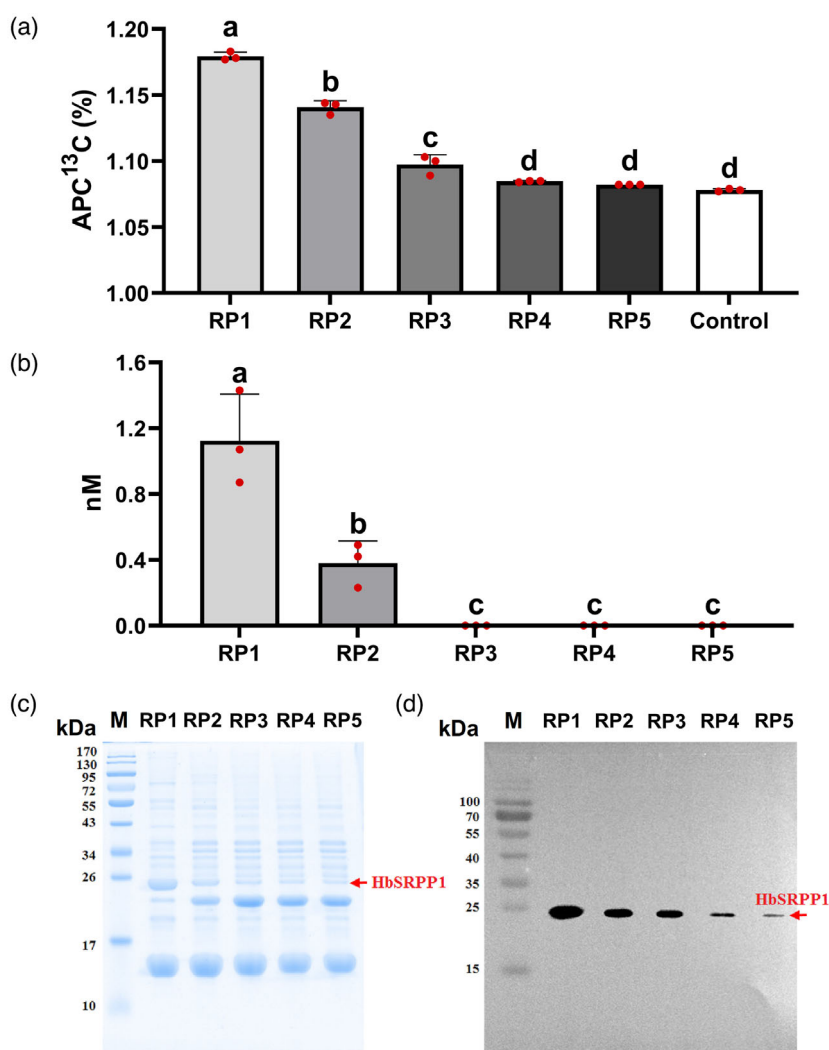


Figure 5. Rubber biosynthesis activity and FPS and HbSRPP1 abundance in RPs of different sizes. (a) Rubber biosynthesis activity of the RPs with different sizes. (b) FPS abundance in the RPs with different sizes. (c) SDS-PAGE profiles of different size RPs. (d) Western blot analyses with monoclonal antibodies raised against HbSRPP1. The HbSRPP1 protein is indicated by the arrow. RP1, RPs with VMD < 0.15 μm ; RP2, RPs with VMD about 0.3 μm ; RP3, RPs with VMD about 0.5 μm ; RP4, RPs with VMD about 0.7 μm ; RP5, RPs with VMD > 1.0 μm . Control, the reaction was performed in 400 μl normal reaction buffer containing 30 μl resuspended RPs with 25 mM EDTA added for immediate reaction termination. M, molecular markers. Data are presented as means \pm SE. One-way analysis of variance and the Student–Newman–Keuls test were performed to identify significant differences between groups. Different letters indicate significant differences ($P < 0.05$, $n = 3$). FPS, farnesyl pyrophosphate synthase; RPs, rubber particles; VMD, volume mean diameter; APC-¹³C, atom percentage of ¹³C.

promoter. Furthermore, the luciferase (LUC) activity in tobacco (*Nicotiana benthamiana*) leaves harboring *HbERE**EBP1* or the *MYB2-like* gene and *LUC* driven by the *HbFPS1* promoter was significantly higher than in leaves harboring *LUC* alone (Figure 8d,e). These findings confirm that HbERE-EBP1 and MYB2-like promote *HbFPS1* transcription by binding to its promoter.

Relative expression changes of *HbFPS1* and its transcription regulators *MYB2-like* and *HbERE**EBP1*

Relative expression analysis of different rubber tree tissues indicated that the *MYB2-like* gene was expressed in both bark and latex, while *HbERE**EBP1* was expressed in bark, leaves,

and latex (Figure 9a). *MYB2-like* has a similar expression pattern to *HbFPS1* and was significantly downregulated in T4 latex samples and the corresponding bark samples. However, both RNA-seq and RT-qPCR assays showed no differences in expression of *HbERE**EBP1* in the latex or bark between TPD-affected trees and healthy trees (Figures 8b and 9b,c).

DISCUSSION

TPD seriously affects the NR yield and quality of rubber trees (Putranto & Montoro, 2016; Zhang et al., 2017). Previous studies investigated the molecular mechanisms of TPD using suppression subtractive hybridization and transcriptome sequencing analysis (Li et al., 2010, 2016; Liu et al., 2015).

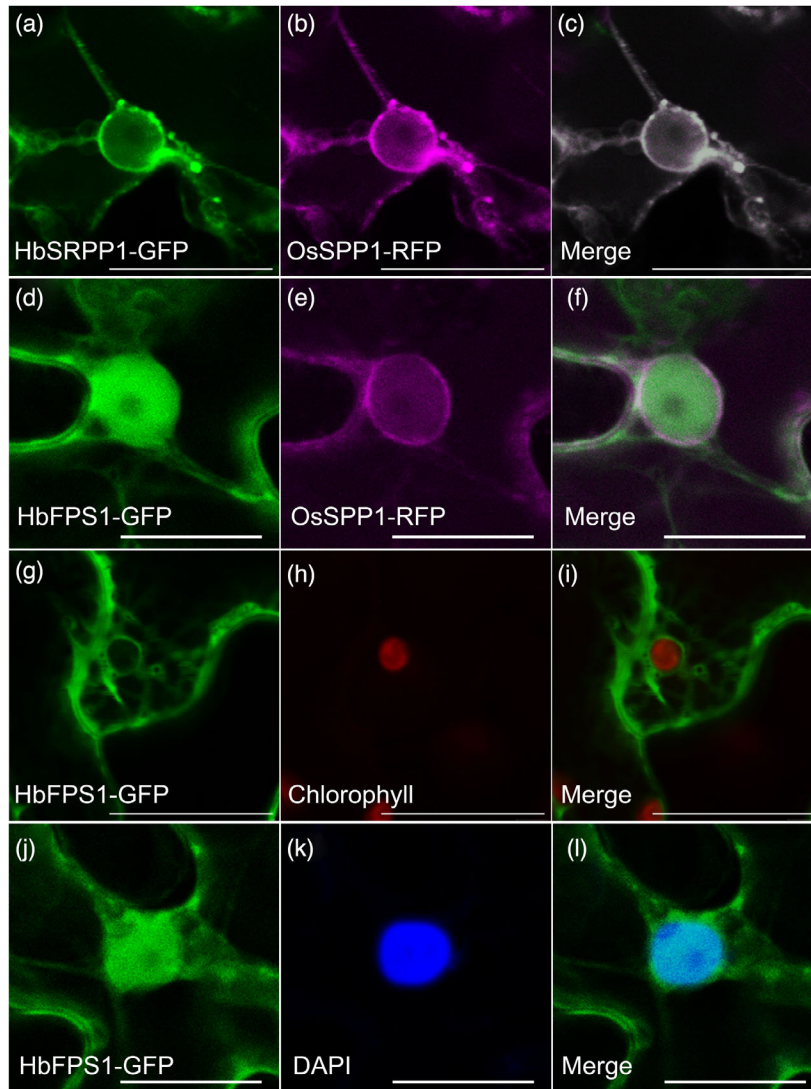


Figure 6. Subcellular localization of HbFPS1 and HbSRPP1 in *N. benthamiana* leaf epidermal cells. (a–c) HbSRPP1-GFP is shown in green and OsSPP1-RFP is shown in pink. (d–f) HbFPS1-GFP is shown in green and OsSPP1-RFP is shown in pink. (g–i) HbFPS1-GFP is shown in green and chlorophyll autofluorescence is shown in red. (j–l) HbFPS1-GFP is shown in green and nuclei stained with DAPI are shown in blue. Scale bars: 25 μm .

However, no study has investigated the rubber biosynthesis activity and quality in TPD-affected trees. Our study confirmed that TPD-affected trees had significantly lower rubber biosynthesis activity and higher NR molecular weight compared to healthy trees (Figure 1i,j). On this basis, we carried out latex transcriptome sequencing and iTRAQ-based proteome analysis of healthy trees and trees with different degrees of TPD, obtaining a total of 2330 DEGs and 272 DAPs. These DEGs and DAPs were significantly enriched in 28 KEGG pathways, which were mainly related to energy metabolism, carbohydrate metabolism, lipid metabolism, ROS scavenging, PCD, and signal transduction/information processing (Figure 2c; Table S4). Thus, it can be concluded that TPD affects energy, carbohydrate, and lipid metabolism, as well as ROS scavenging, PCD, and signal transduction/

information processing, which is consistent with the physiological parameters of latex from healthy and TPD-affected trees and in agreement with previous studies (Chen et al., 2003; de Faÿ, 2011; Li et al., 2010, 2016; Peng et al., 2011; Putranto & Montoro, 2016; Venkatachalam et al., 2009; Zhang et al., 2017). Notably, the correlation between DEGs and DAPs was very poor ($r = 0.024$ in T2_H and $r = 0.104$ in T4_H), indicating that the protein abundance in the latex of TPD-affected trees may be significantly affected by post-translational modifications and splicing events (Pandey & Mann, 2000). Our study further confirms that post-transcriptional modifications and silencing affect important biological pathways of laticiferous cells (Leclercq et al., 2020). As a result, studying the mechanisms underlying TPD using only transcript-level analyses can lead to misleading conclusions.

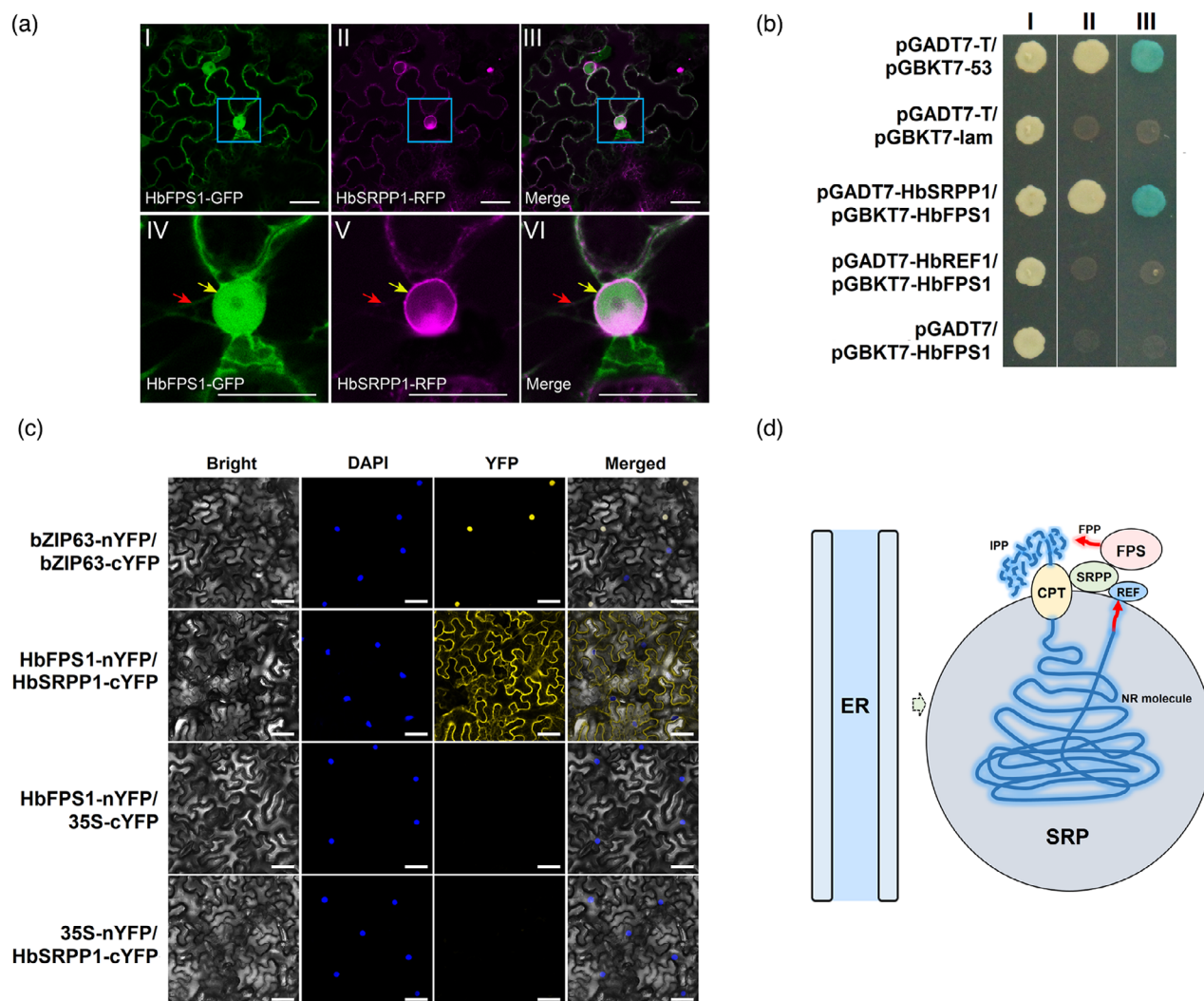


Figure 7. Co-expression and physical interaction analyses of HbFPS1 with HbSRPP1. (a) Co-expression analyses of HbFPS1 with HbSRPP1. HbSRPP1-GFP is shown in green and HbSRPP1-RFP is shown in pink. The nuclear envelope and the ER are indicated by yellow and red arrows, respectively. IV–VI represent magnified images of the areas identified by the squares in I–III. Scale bars: 25 μ m. (b) Physical interaction analyses between HbREF1, HbSRPP1, and HbFPS1 by individual Y2H assays. (I) SD/–Leu–Trp. (II) QDO. (III) QDO/X- α -gal. (c) HbFPS1–HbSRPP1 interaction analysis by BiFC assay. The bZIP63 transcription factor was used as a positive control. The empty pairs (n-YFP and c-YFP) were used as negative controls. YFP fluorescence was detected under a confocal laser microscope. Scale bar = 25 μ m. (d) Possible model for RP biogenesis and protein–protein interacting pattern among the rubber biosynthesis-related proteins. QDO, quadruple dropout plates (SD/–Ade–His–Leu–Trp); RP, rubber particle; ER, endoplasmic reticulum; SRP, small rubber particle; CPT, *cis*-prenyltransferase; SRPP, small rubber particle protein; FPS, farnesyl pyrophosphate synthase; FPP, farnesyl pyrophosphate; IPP, isopentenyl pyrophosphate; NR, natural rubber.

Rubber is synthesized in the laticifers, which are non-photosynthetic tissues that are particularly susceptible to oxidative stress (de Faÿ et al., 1989). Of the 272 DAPs identified by iTRAQ-based proteome analysis, 17 were associated with ROS metabolism, of which 14 were downregulated (Table S8). The DAP analysis results and the physiological parameters of decreased RSH content indicated that alterations in ROS metabolic capacity were one of the crucial events in the latex of TPD-affected trees. ROS metabolism is key for NR production, rubber quality, and tolerance to biotic and abiotic stresses (Zhang et al., 2017). ROS production can be significantly

augmented due to environmental and harvesting stress and metabolic activities essential for latex regeneration between two tapplings. Therefore, rubber tree overexploitation with high-frequency rubber tapping and excessive ET stimulation can lead to decreased RSH content, excessive ROS accumulation, and, ultimately, TPD occurrence (Putranto et al., 2015). This is supported by our results, as we observed a decrease in the abundance of ROS metabolism-related proteins and in RSH content in the latex of TPD-affected trees. Excessive ROS accumulation caused by decreased RSH levels in the laticiferous cells of TPD-affected trees mainly leads to membrane damage,

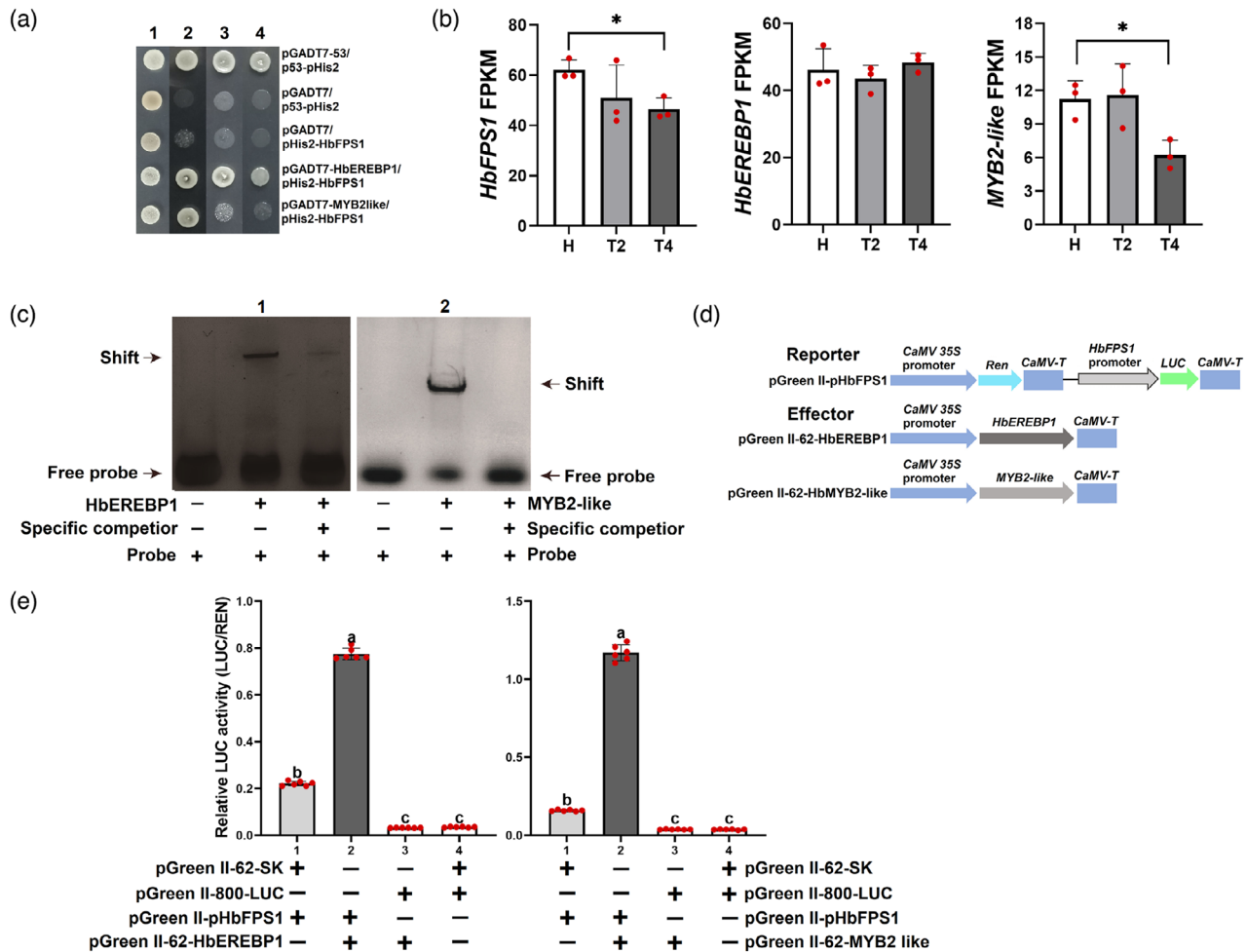


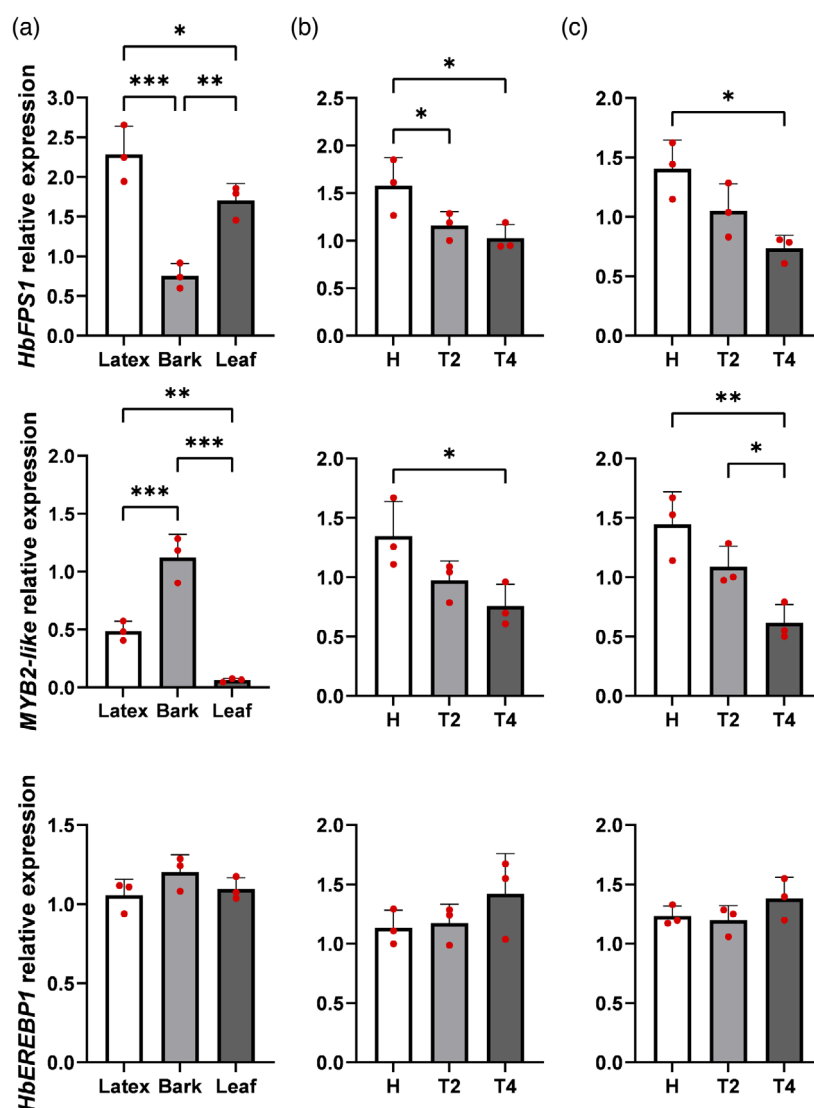
Figure 8. Validation of *HbFSP1* transcription regulators. (a) Activation of the *HbFSP1* promoter in yeast by the HbEREBP1 and MYB2-like proteins. (1) SD/-Leu/-Trp. (2) TDO/80 mm 3-AT. (3) TDO/120 mm 3-AT. (4) TDO/160 mm 3-AT. (b) *HbFSP1*, *HbEREBP1*, and *MYB2-like* FPKM values in the latex of TPD-affected and healthy trees. *FDR < 0.05. (c) Physical binding of HbEREBP1 (1) and MYB2-like (2) to the *HbFSP1* promoter was shown by electrophoretic mobility shift assays. The symbols + and - indicate differences in reaction buffer components. (d) Schematic representation of the vector structure for the Dual-LUC assays. (e) Transient transcriptional activity assays of HbEREBP1 and MYB2-like on the *HbFSP1* promoter. Data are presented as means \pm SE. One-way analysis of variance and the Student-Newman-Keuls test were performed to identify significant differences between groups. Different letters indicate significant differences ($P < 0.05$, $n = 6$). TDO, triple dropout plates (SD/-His-Leu-Trp); TPD, tapping panel dryness.

lutoid bursting, and subsequent *in situ* latex coagulation (Junaidi et al., 2022). However, this is not the major reason for the decline in rubber biosynthesis activity in TPD-affected trees.

It has been proposed that TPD could affect rubber biosynthesis by downregulating rubber biosynthesis-related genes (Li et al., 2010, 2016; Liu et al., 2015). In the present study, only *HbFSP1* was highly expressed among the DEGs related to rubber biosynthesis, and its transcript and protein levels were both progressively reduced with TPD development (Figure 2d; Tables S5 and S6). Three FPS genes have been discovered in the rubber tree genome (Tang et al., 2016), and only *HbFSP1*, involved in a branching pathway (ko00900, terpenoid backbone biosynthesis) of terpenoid backbone biosynthesis (ko09109) in plants, is highly expressed in rubber tree latex (Table S5). HbFSP1 is

a key enzyme in rubber biosynthesis (Men et al., 2019). Tanaka et al. (1996) suggested that the direct initiator of rubber biosynthesis may be a C15 APP consisting of two *trans*-isoprene units modified on dimethylallyl. Such units include FPP or FPP in which dimethylallyl groups are modified after polymerization. Several *in vitro* studies on rubber biosynthesis have shown a variety of APPs, such as DMAPP, GGP, and GGPP, which are able to initiate rubber chain elongation (Cornish, 2001). However, *in vitro* rubber synthesis assays with WRPs as cofactor clearly showed that FPP is the most efficient in rubber biosynthesis initiation (Xie et al., 2008). In the present study, we first confirmed that the rubber biosynthesis activity of TPD-affected trees was decreased and further confirmed that the FPS and FPP contents in the latex of TPD-affected trees were reduced. Obviously, due to the significantly decreased

Figure 9. Relative expression of *HbFPS1* and the transcription factor-encoding genes *MYB2-like* and *HbEREBP1* in (a) different rubber tree tissues, (b) the latex of TPD-affected and healthy rubber trees, and (c) the barks of TPD-affected and healthy rubber trees. Data are presented as means \pm SE. One-way analysis of variance and the Student–Newman–Keuls test were performed to identify significant differences between groups. * $P < 0.05$, ** $P < 0.01$, *** $P < 0.001$, $n = 3$. TPD, tapping panel dryness.



abundance of HbFPS1 in the latex, the content of its catalytic product FPP is correspondingly decreased, which reduces the initiation of NR chain synthesis and thus affects rubber biosynthesis in TPD-affected trees.

To confirm the influence of decreased HbFPS1 abundance or FPP content on rubber biosynthesis, we analyzed the effects of FPP and HbFPS1 on rubber biosynthesis efficiency with *in vitro* WRPs and further investigated the impact of FPP, HbFPS1, or FPS inhibitors on rubber biosynthesis efficiency in latex. These experiments not only repeatedly verified the impact of FPP on rubber biosynthesis efficiency in the assays without other APPs (*in vitro* rubber biosynthesis assays with WRPs as cofactor), but also further confirmed the effects of HbFPS1 and its catalytic product FPP on rubber biosynthesis efficiency in assays with multiple APPs (using latex containing a variety of APPs as cofactors). Therefore, HbFPS1 and FPP content or FPS enzyme activity are positively correlated with rubber

biosynthesis, demonstrating that HbFPS1 downregulation is causal for the decreased rubber biosynthesis activity in the latex of TPD-affected trees.

Moreover, we found that the molecular weight of rubber in TPD-affected trees is higher than that of rubber in healthy trees. Previous studies using *in vitro* rubber biosynthesis assays with WRPs as cofactor suggested that initiation and polymerization rates and biopolymer molecular weight were affected by the GPP or FPP content (Cornish, 2001). Increasing GPP or FPP concentrations increased the rubber biosynthesis rate and the number of newly initiated rubber molecules. However, GPP or FPP could decrease the rubber molecular weight by competition with the APP end of elongating rubber molecules for the APP binding site (Cornish, 2001; Rojruthai et al., 2010). In the present study, we followed Cornish et al. (2000) to analyze the effects of FPP and HbFPS1 on rubber molecular weight using *in vitro* WRPs. We additionally analyzed the

impacts of FPP, HbFPS1, and FPS inhibitors on the molecular weight of rubber using total latex. We confirmed the effects of FPP and FPS on the molecular weight of rubber in an experimental system mimicking the intracellular environment of a laticifer. Our results indicate that the downregulation of HbFPS1 is potentially responsible for the increased molecular weight of rubber in TPD-affected trees. This is the first *in vivo* observation in rubber trees that a decrease in FPP or FPS content leads to an increase in rubber molecular weight.

Regarding the relationship between rubber biosynthesis activity and RP size, we found that the abundance of SRPs (VMD < 0.3 μm) with high rubber biosynthesis activity (Figure 5a) in TPD-affected tree latex is significantly higher compared to healthy trees (Figure 1g). However, the rubber biosynthesis activity of TPD-affected tree latex was significantly reduced compared to that of healthy trees (Figure 1i). In light of these results, we suggest that the decreased abundance of HbFPS1 in latex may be one of the main reasons for the physiological disorder of TPD-affected trees. HbFPS1 is a soluble *trans*-prenyl transferase expressed in laticifer cytoplasm (Figure 6) (Adiwilage & Kush, 1996; Cornish, 1993). We discovered that HbFPS1 could be recruited from the cytoplasm to RPs by HbSRPP1 through protein–protein interactions (Figure 7) and mainly relocates on SRPs with particle sizes smaller than 0.15 μm (Figure 5b–d). The attachment of these enzymes to the membrane surface of SRPs can facilitate FPP production to initiate the rubber synthesis-related metabolic channeling, which is fulfilled by a protein complex that functions as the NR biosynthesis machinery on SRPs (Brown et al., 2017; Niephaus et al., 2019; Yamashita et al., 2016; Yamashita & Takahashi, 2020). It was observed in cytological studies that RP size gradually increases with increasing amounts of rubber molecules synthesized and packed in the RPs (Wu & Hao, 1990). Therefore, a lower abundance of HbFPS1 might directly lead to a decrease in rubber biosynthesis activity and affect RP development in TPD-affected trees.

Given that changes in HbFPS1 abundance significantly affect rubber biosynthesis in latex, we further screened and validated upstream regulators of *HbFPS1*. Two transcription factors (HbEREBP1 and MYB2-like) that may regulate *HbFPS1* were assessed. HbEREBP1 belongs to the APETALA2/ethylene response factor (AP2/ERF) superfamily, whose members are critical in plant ET signal transduction. Several AP2/ERF members are highly accumulated in laticifers and produced in response to ET stimulation (Nie et al., 2016; Putranto & Montoro, 2016). In the present study, both RNA-seq and RT-qPCR assays showed no expression differences of *HbEREBP1* in the latex between TPD-affected trees and healthy trees, suggesting that HbEREBP1 may not be involved in *HbFPS1* downregulation in TPD-affected trees. MYB transcription factors are

involved in plant secondary metabolic pathway regulation, which typically provides regulatory specificity for a given target pathway in secondary metabolism by binding to specific *cis*-regulatory elements in gene promoters (Chezem et al., 2016). Rubber biosynthesis is a branch of the isoprenoid pathway and MYB transcription factors may play key regulatory roles. Wang et al. (2017) identified 44 *H. brasiliensis* MYB transcription factors through latex transcriptome analysis. Among those, HbIMYB19 and HbIMYB44 promoted expression of rubber biosynthesis-related genes. In addition, MYB transcription factors are closely linked to rubber tree TPD. For example, *HbMYB1* downregulation in the bark tissue of TPD-affected trees was associated with PCD (Chen et al., 2003; Peng et al., 2011). In the present study, we identified a novel gene encoding a latex-expressed MYB transcription factor, *MYB2-like* (Figure S5), which could promote *HbFPS1* expression (Figure 8 e). It also exhibited similar expression patterns with *HbFPS1* (Figures 8b and 9), suggesting that it may be directly involved in the TPD-mediated downregulation of *HbFPS1*. Thus, downregulation of *HbFPS1* in the latex of TPD-affected trees may be caused by the upstream downregulation of transcription factors such as MYB2-like, whose reduced binding to the *HbFPS1* promoter results in its downregulation. Our study significantly enriches our understanding of pivotal node genes involved in the regulation of rubber biosynthesis, shedding light on the molecular mechanisms underlying the reduction in rubber yield of TPD-affected rubber trees and potentially providing targets for the molecular breeding of rubber trees with reduced TPD incidence.

EXPERIMENTAL PROCEDURES

Plant materials

Hevea brasiliensis clone Reyan 73397 was grown at the experimental plantation of the Chinese Academy of Tropical Agricultural Sciences (Hainan, China). Trees were 13 years old at the time of sampling. The harvesting system was used for 3 years before sampling. Sampling was performed by half spiral tapping (S/2) once every three days. 1.0% Ethephon (2-chloroethyl phosphonic acid, an ethylene-releasing compound) was applied to stimulate latex yield once every five tappings. In this study, the latex taken from 12 healthy trees with normal latex flow was designated as 'H', the latex from 12 TPD-affected trees showing partial latex flow along more than 3/4 of the length of the tapping cut was designated as 'T2', and the latex from 12 TPD-affected trees with latex flow along less than 1/4 of the length of the tapping cut was designated as 'T4' (Figure S1).

Measurement of latex physiological parameters and rubber biosynthesis activity

A 5-ml latex aliquot per tree was placed on ice 5 min after tapping for immediate analysis. For rubber molecular weight determination, 0.2 ml of latex from each tree was dried, and then 30 mg of dry rubber was dissolved in 10 ml tetrahydrofuran (THF) and filtered with a 0.45 μm Minisart SRP 25 filter (Sartorius, Gottingen,

Germany). The molecular weight of NR was determined by gel permeation chromatography (GPC). The GPC system includes a Waters 1515 isocratic HPLC pump equipped with a 2414 refractive index detector (RID) (Waters Corporation, Milford, MA, USA) and Styragel HR5 columns (Waters Corporation). *cis*-1,4-Polyisoprene (Agilent Technologies, Santa Clara, CA, USA) was used as a standard sample for molecular weight calibration. GPC was carried out using 30 μ l of rubber solution at 40°C with THF as eluent at a flow rate of 1.0 ml min⁻¹, monitored by RID. The latex rubber biosynthesis activity in NR samples was determined by calculating the ¹³C content relative to the total carbon (¹³C + ¹²C) content and was expressed as atom percent (APC) according to Deng et al. (2018). The average RP size (VMD) was measured by an LA-960S laser particle analyzer (Horiba, Kyoto, Japan). The NR yield, RSH content, and sucrose content were determined as previously described (Nie et al., 2016). The Mg²⁺ content of C-serum in latex was measured by the ethylene diamine tetraacetic acid (EDTA) titration method. Pi content was determined according to Taussky and Shorr (1953).

Total RNA and protein extraction

Three independent biological replicates were collected for each group (labeled H_1, H_2, H_3, T2_1, T2_2, T2_3, T4_1, T4_2, and T4_3). For each biological replicate, latex (10 ml per tree), bark, and leaves (1 g per tree) were collected equally from four trees and pooled. The total RNA was extracted from the latex (Nie et al., 2015), bark, and leaf (Nie et al., 2018). RNA quantity and quality were determined using a NanoDrop 2000 spectrophotometer (Thermo Fisher Scientific, Waltham, MA, USA) and a Bioanalyzer Chip RNA 7500 Series II (Agilent Technologies, Santa Clara, CA, USA). RP protein was extracted according to Dai et al. (2013). Total protein was extracted from the latex as previously described (Dai et al., 2016).

RP preparation and rubber biosynthesis *in vitro* assays

The WRPs were prepared according to the method of Siler and Cornish (1993). To isolate the different size RPs, 400 ml of fresh latex harvested from healthy trees was centrifuged at 10 000 *g* for 30 min to collect the rubber cream containing the LRPs in the upper layer. At the same time, the SRPs remained in the water layer. The collected LRPs were resuspended in 400 ml of Tris-HCl (pH 7.5) and then filtered with sterile gauze. The resuspended LRPs were centrifuged at 1000 *g* for 60 min to collect the rubber cream termed fraction RP5 (the largest RPs with VMD > 1.0 μ m) of the RPs. The remaining water layer with low turbidity was centrifuged sequentially at 2000 *g* and 6000 *g* for 60 min. The upper rubber cream from each centrifuge step was collected as fraction RP4 (VMD about 0.7 μ m) and fraction RP3 (VMD about 0.5 μ m), respectively. The remaining separated water layer containing SRPs was further sequentially centrifuged at 18 000 *g* and 50 000 *g* for 45 min. The rubber cream from each centrifugation step was collected as fraction RP2 (VMD about 0.3 μ m) and fraction RP1 (the smallest RPs with VMD < 0.15 μ m), respectively. The collected RP1–5 fractions were resuspended in two volumes of Tris-HCl (pH 7.5) and filtered with gauze for subsequent experiments.

In the rubber biosynthesis efficiency assays using *in vitro* RPs as cofactor, the resuspended RPs (30 μ l) were mixed with 400 μ l of reaction buffer containing 1 mM (2-¹³C)IPP (¹³C-IPP) (Toronto Research Chemicals, North York, ON, Canada), 2 mM MgSO₄, 1 mM DTT, 60 mM KCl, 5 μ M ATP, and 20 μ M FPP in 0.1 M Tris-HCl (pH 7.5). The reaction conditions and detection methods for rubber synthesis efficiency were similar to those described by Deng et al. (2018), and the results are expressed as APC values.

Approximately 3 mg of the synthesized NR was dissolved in 500 μ l THF, and its molecular weight was measured by GPC according to the abovementioned method. Three biological replicates were used for all analyses. The rubber biosynthesis efficiency assays, using *in vitro* latex as cofactor, were performed as described previously (Deng et al., 2018).

Identification of DEGs from the latex of healthy and TPD-affected trees

RNA-seq was performed according to Li et al. (2016). The clean reads from each biological replicate were mapped to the reference genome (accession no. PRJNA394253) by TopHat2 (version 2.0.3.12). The expected number of fragments per kilobase of transcript sequence per millions of base pairs sequenced (FPKM) method was applied to calculate unigene expression using RSEM software (v1.2.15). DESeq software (1.6.3) was used to identify DEGs based on each unigene read count from samples H, T2, and T4 with FDR < 0.05 as a threshold.

Identification of DAPs by iTRAQ technology

The iTRAQ assays were performed as previously described (Dai et al., 2016). Sample H from healthy trees was labeled with iTRAQ tag 118, while samples T2 and T4 from TPD-affected trees were labeled with tags 119 and 121, respectively. Proteins were identified and quantified using SEQUEST software integrated with Proteome Discoverer 2.1 (Thermo Fisher Scientific) with the *H. brasiliensis* genome database (accession no. PRJNA394253) as a reference. Protein functional classification and pathway annotation were conducted against the COG and KEGG databases. DAPs were defined as the proteins with fold change > 1.2 or fold change < 0.85 (mean value of all compared groups) and *P* < 0.05 (*t*-test for all comparisons) between samples H and T2 or samples H and T4.

KEGG pathway enrichment analyses and RT-qPCR

The KEGG pathway enrichment analyses of DEGs and DAPs were performed as previously described (Li et al., 2016). In total, 30 genes that were identified and quantified in the transcriptome and proteome assays were randomly selected for verification by RT-qPCR. Ten of them were identified as both DEGs and DAPs, and 20 were identified as DAPs. RT-qPCR analysis was performed according to Nie et al. (2016). The relative gene expression levels were calculated using the *YLS8* gene (NCBI Reference Sequence: HQ323250.1) as the internal reference for normalization. The primers for the selected genes were designed using Vector NTI software (Thermo Fisher Scientific) (Table S7).

FPS and FPP content analysis in the latex

For FPS content measurement, 100 μ l of latex or 100 μ g of RPs was immediately mixed with 100 μ l of 0.1 M Tris-HCl buffer (pH 7.5) on ice, and the FPS content was measured by the Plant Farnesyl Pyrophosphate Synthase ELISA kit following the user manual (JIANGLAI Biological, Shanghai, China) using a Multiskan™ FC Microplate Photometer (Thermo Fisher Scientific). For FPP content determination of latex samples, the method of Zhang et al. (2015) was followed with modifications. Latex (5 ml) was immediately mixed in a 50-ml centrifuge tube with 5 ml of 36 mM phosphate buffer (pH 7.0) and 10 U alkaline phosphatase (Promega Corporation, Madison, WI, USA), followed by incubation for 30 min at 37°C. Then, 30 ml of *n*-hexane was added to the reaction and mixed thoroughly. The mixture was placed at room temperature for 30 min and then centrifuged at 12 000 *g* for 20 min. Subsequently, the supernatant was mixed with 15 ml of absolute

ethanol and centrifuged at 10 000 *g* for 10 min. The centrifuged supernatant was filtered through a 0.2 µm Minisart SRP 25 filter (Sartorius, Gottingen, NI, Germany) and then concentrated under a stream of nitrogen (14 psi) to approximately 20 µl. It was finally diluted with *n*-hexane to a final volume of 200 µl. Then, 1 µl of the sample was injected into the GC column in splitless mode. The metabolite chemical constituents were detected using a TSQ8000 Evo gas chromatograph/mass spectrometer (Thermo Fisher Scientific) with 70 eV of electron impact ionization. Samples were introduced through a DB-5 MS capillary column of 30 m × 0.25 µm × 250 µm (Thermo Fisher Scientific). The initial column temperature was 70°C, which was held for 3 min and then increased to 300°C at a rate of 10°C min⁻¹, with a final hold time of 5 min. Helium was used as the carrier gas with a linear velocity of 1 ml min⁻¹. The MS transfer line and ion source temperatures were 300°C and 230°C, respectively. The scanning range was 50–650 *m/z*. Relative quantitative analysis was performed using TraceFinder 4.1 software according to Yuan et al. (2019).

HbFPS1 expression in *Escherichia coli*

The *HbFPS1* open reading frame (ORF) was synthesized by Sangon Biotech (Shanghai) Co., Ltd. (China). It was cloned into the expression vector pET22b (+) (Novagen, Madison, WI, USA) at the *Xho*I and *Mlu*I sites to generate the pET22b-HbFPS1 construct and introduced in *E. coli* BL21 (DE3) (Novagen). Protein biosynthesis was induced with 0.2 mM isopropyl β-D-thiogalactopyranoside (IPTG) at 37°C for 4 h. The expressed protein was identified by Western blot analysis using 6×His Tag Monoclonal Antibodies (Thermo Fisher Scientific) and purified using the HisPUR Ni-NTA Spin Purification Kit according to the manufacturer's instructions (Thermo Fisher Scientific).

Y2H, subcellular localization, co-expression, BiFC, and Western blot assays

For Y2H assays, the ORFs of *HbFPS1*, *HbREF1* (XM_021797910.1), and *HbSRPP1* (XM_021797905.1) were synthesized by Sangon Biotech (Shanghai) Co., Ltd. and inserted in the vectors pGADT7 and pGBKT7. The Y2H, BiFC, and Western blot assays were performed as described by Deng et al. (2018). The subcellular localization and co-expression assays were performed as previously described (Brown et al., 2017). The ER of the *N. benthamiana* leaf epidermal cells was visualized by OsSPP1-RFP.

Y1H, EMSA, and Dual-LUC assays

The *HbFPS1* promoter fragment (1066 bp) was synthesized according to its published sequence (Wang et al., 2017) by Sangon Biotech (Shanghai) Co., Ltd. and inserted in the vector pHis2.1 to generate the bait vector pHis-pHbFPS1. Total RNA was extracted from the latex and was mixed in equal proportions from samples H, T2, and T4 for cDNA library construction. The cDNA library was constructed using the Matchmaker Gold Yeast One-Hybrid Library Screening System Kit (Clontech, Mountain View, CA, USA) and screened according to the Matchmaker Gold Y1H System protocol (Clontech). Positive colonies were verified by individual Y1H assays, according to Deng et al. (2018). The *HbEREBP1* and *MYB2-like* gene ORFs were synthesized and cloned into the expression vector pET28a (+) (Novagen). The constructed expression vectors were introduced into *E. coli* strain BL21 to produce the HbEREBP1 and MYB2-like recombinant proteins. EMSA was performed using the LightShift Chemiluminescent EMSA Kit (Thermo Fisher Scientific) following the manufacturer's instructions. The EMSA probe sequences are listed in Table S7. The *HbFPS1* promoter fragment was synthesized and inserted in the reporter vector pGreenII 0800-

LUC. The *HbEREBP1* and *MYB2-like* ORFs were synthesized and cloned into the effector vector pGreenII 62-SK. Tobacco (*N. benthamiana*) was sown and grown at 25°C in a 16/8 h light/dark photoperiod for approximately 6 weeks before being used for Dual-LUC assays. The Dual-Luciferase Reporter Assay System kit (Promega Corporation) was used to perform the Dual-LUC assays. Six biological replicates were conducted for each combination.

Statistical analysis

SPSS version 22.0 (IBM Corp., Armonk, NY, USA) was used for statistical analyses. One-way analysis of variance and the Student–Newman–Keuls test were used for comparisons between multiple groups.

ACKNOWLEDGMENTS

This study was supported by funds from the National Key Research and Development Program of China (2019YFD1000502, 2018YFD1000502), the National Natural Science Foundation of China (31770642), the High-level Talent Project of Hainan Provincial Natural Science Foundation of China (2019RC328), and the Central Public-interest Scientific Institution Basal Research Fund for the Chinese Academy of Tropical Agricultural Sciences (1630022020006).

AUTHOR CONTRIBUTIONS

Conceived and designed the experiments: ZYN, RZZ, and LFY. Performed the experiments: ZYN, GJK, DY, and HDQ. Analyzed the data: ZYN. Contributed reagents/materials/analysis tools: ZYN, GJK, DY, and HDQ. Wrote the paper: ZYN and RZZ.

CONFLICT OF INTEREST

The authors have no conflicts of interest to declare.

DATA AVAILABILITY STATEMENT

The sequencing reads and the assembled sequences were submitted to the NCBI TSA project under BioProject ID PRJNA752925 (SRA ID: SRS9707301–SRS9707309). The MS proteomics data were deposited to the ProteomeXchange Consortium via the PRIDE partner repository under dataset identifier PXD027892. All other relevant data can be found within the manuscript and its supporting materials.

SUPPORTING INFORMATION

Additional Supporting Information may be found in the online version of this article.

Figure S1. Images of healthy and TPD-affected rubber trees. (a) A healthy rubber tree with normal latex flow. (b) A TPD-affected rubber tree with latex flow from 3/4 or more of the tapping panel. (c) A TPD-affected rubber tree with latex flow from 1/4 or less of the tapping panel. TPD, tapping panel dryness.

Figure S2. Transcript levels and protein abundance in healthy and TPD-affected rubber trees. (a) Venn diagram of DEGs and DAPs. (b) Shared DEGs and DAPs between groups. P24, shared DAPs between T2_H and T4_H; G24, shared DEGs between T2_H and T4_H; P2G2, genes in T2_H whose associated transcript levels and protein abundance exhibited similar trends; P4G4, genes in T4_H whose associated transcript levels and protein abundance

exhibited similar trends. (c) Comparison of changes in transcript and protein levels of DEGs and DAPs. (d) Correlations between transcript levels and protein abundance in DEGs and DAPs from T2_H. (e) Correlations between transcript levels and protein abundance in DEGs and DAPs from T4_H. DEGs, differentially expressed genes; DAPs, differentially abundant proteins.

Figure S3. Validation of DEGs and DAPs using RT-qPCR. RT-qPCR analyses of healthy (H) and TPD-affected rubber trees (T2 and T4). *YLS8* was used as a reference gene. The heatmap of the 30 selected genes was drawn using log₂(fold change) values from the RT-qPCR, RNA-seq, and iTRAQ-based proteome data. DEGs, differentially expressed genes; DAPs, differentially abundant proteins; TPD, tapping panel dryness.

Figure S4. *E. coli* expression and purification of HbFPS1. (a) Heterologous expression of *HbFPS1* in *E. coli*. (I) Molecular markers. (II) *E. coli* cells harboring pET22b-HbFPS1 not induced. (III) *E. coli* cells harboring pET22b-HbFPS1 induced by 0.2 mM IPTG at 37°C after 4 h. (b) HbFPS1 purification. (I) Molecular markers. (II) Purified HbFPS1 fusion protein. (c) Western blot of HbFPS1 fusion protein. (I) Molecular markers. (II) HbFPS1 fusion protein.

Figure S5. Phylogenetic analysis of *HbIMYBs* and *MYB2-like* based on MUSCLE alignments and the Maximum Likelihood method with MEGA 6.0. The internal branch support was estimated with 1000 bootstrap replicates. For details on the *HbIMYB* sequences, see Wang *et al.* (2017).

Table S1. Transcriptome sequencing quality assessment and sequence alignment results.

Table S2. DEG characteristics between TPD-affected and healthy rubber tree latex.

Table S3. DAP characteristics between TPD-affected and healthy rubber tree latex.

Table S4. Significantly enriched KEGG pathways among the DEGs and DAPs between TPD-affected and healthy rubber tree latex.

Table S5. Expression changes of genes involved in rubber biosynthesis based on RNA-seq.

Table S6. Abundance changes of proteins involved in rubber biosynthesis based on iTRAQ-based proteomic analysis.

Table S7. List of primers used in this study.

Table S8. Variation in abundance of DAPs related to ROS metabolism based on iTRAQ proteomic analysis.

REFERENCES

- Adiwilage, K. & Kush, A.** (1996) Cloning and characterization of cDNA encoding farnesyl diphosphate synthase from rubber tree (*Hevea brasiliensis*). *Plant Molecular Biology*, **30**, 935–946.
- Brown, D., Feeny, M., Ahmadi, M., Lonoce, C., Sajari, R., Di Cola, A. *et al.*** (2017) Subcellular localization and interactions among rubber particle proteins from *Hevea brasiliensis*. *Journal of Experimental Botany*, **68**, 5045–5055.
- Chen, S.C., Peng, S.Q., Huang, G.X., Wu, K.X., Fu, X.H. & Chen, Z.Q.** (2003) Association of decreased expression of a Myb transcription factor with the TPD (tapping panel dryness) syndrome in *Hevea brasiliensis*. *Plant Molecular Biology*, **51**, 51–58.
- Chezem, W.R., Nicole, K. & Clay, N.K.** (2016) Regulation of plant secondary metabolism and associated specialized cell development by MYBs and bHLHs. *Phytochemistry*, **131**, 26–43.
- Chow, K.S., Mat-Isa, M.N., Bahari, A., Ghazali, A.K., Alias, H., Mohd-Zainuddin, Z. *et al.*** (2012) Metabolic routes affecting rubber biosynthesis in *Hevea brasiliensis* latex. *Journal of Experimental Botany*, **63**, 1863–1871.
- Chrestin, H.** (1989) Biochemical aspects of bark dryness induced by overstimulation of rubber trees with Ethrel. In: d'Auzac, J., Jacob, J.L. & Chrestin, H. (Eds.) *Physiology of rubber tree latex*. Boca Raton, FL: C.R.C. Press, pp. 431–441.
- Cornish, K.** (1993) The separate roles of plant *cis* and *trans* prenyl transferases in *cis*-1,4-polyisoprene biosynthesis. *European Journal of Biochemistry*, **218**, 267–271.
- Cornish, K.** (2001) Similarities and differences in rubber biochemistry among plant species. *Phytochemistry*, **57**, 1123–1134.
- Cornish, K., Castillon, J. & Scott, D.J.** (2000) Substrate-dependent rubber molecular weight regulation, *in vitro*, in plant species that produce high and low molecular weights *in vivo*. *Biomacromolecules*, **1**, 632–641.
- Dai, L.J., Kang, G.J., Li, Y., Nie, Z.Y., Duan, C.F. & Zeng, R.Z.** (2013) In-depth proteomic analysis of the rubber particle of *Hevea brasiliensis* (Para rubber tree). *Plant Molecular Biology*, **82**, 155–168.
- Dai, L.J., Kang, G.J., Nie, Z.Y., Li, Y. & Zeng, R.Z.** (2016) Comparative proteomic analysis of latex from *Hevea brasiliensis* treated with Ethrel and methyl jasmonate using iTRAQ-coupled two-dimensional LC-MS/MS. *Journal of Proteomics*, **132**, 167–175.
- d'Auzac, J. & Jacob, J.L.** (1989) The composition of latex from *Hevea brasiliensis* as a laticiferous cytoplasm. In: d'Auzac, J., Jacob, J.L. & Chrestin, H. (Eds.) *Physiology of rubber tree latex*. Boca Raton, FL: C.R.C. Press, pp. 59–96.
- de Fay, E.** (2011) Histo- and cytopathology of trunk phloem necrosis, a form of rubber tree (*Hevea brasiliensis* Muell. Arg.) tapping panel dryness. *Australian Journal of Botany*, **59**, 563–574.
- de Fay, E., Hébant, C. & Jacob, J.L.** (1989) Cytology and cytochemistry of the laticiferous system. In: d'Auzac, J., Jacob, J.L. & Chrestin, H. (Eds.) *Physiology of rubber tree latex*. Boca Raton, FL: C.R.C. Press, pp. 15–27.
- de Fay, E. & Jacob, J.L.** (1989) Anatomical organization of the laticiferous system in the bark. In: d'Auzac, J., Jacob, J.L. & Chrestin, H. (Eds.) *Physiology of rubber tree latex*. Boca Raton, FL: C.R.C. Press, pp. 4–14.
- Deng, X.M., Guo, D., Yang, S.G., Shi, M.J., Chao, J.Q., Li, H. *et al.*** (2018) Jasmonate signalling in the regulation of rubber biosynthesis in laticifer cells of rubber tree, *Hevea brasiliensis*. *Journal of Experimental Botany*, **69**, 3559–3571.
- Deng, Z., Chen, J.S., Leclercq, J., Zhou, Z.Z., Liu, C.R., Liu, H. *et al.*** (2016) Expression profiles, characterization and function of HbTCTP in rubber tree (*Hevea brasiliensis*). *Frontiers in Plant Science*, **7**, 789.
- Epping, J., Deenen, N.V., Niephaus, E., Stolze, A., Fricke, J., Huber, C. *et al.*** (2015) A rubber transferase activator is necessary for natural rubber biosynthesis in dandelion. *Nature Plants*, **1**, 15048.
- Fan, S.W. & Yang, S.Q.** (1984) Cause of disease and hypothesis on tapping panel dryness of *Hevea brasiliensis*. *Hevea brasiliensis. Chinese Journal of Tropical Crops*, **18**, 43–48.
- Faridah, Y., Siti Arija, M.A. & Ghandimathi, H.** (1996) Changes in some physiological latex parameters in relation to over exploitation and onset of induced tapping panel dryness. *Journal of Natural Rubber Research*, **10**, 182–186.
- Gebelin, V., Leclercq, J., Kuswanhadi, Argout, X., Chaidamsari, T., Hu, S.N. *et al.*** (2013) The small RNA profile in latex from *Hevea brasiliensis* trees is affected by tapping panel dryness. *Tree Physiology*, **31**, 1084–1098.
- Hagel, J.M., Yeung, E.C. & Facchini, P.J.** (2008) Got milk? The secret life of laticifers. *Trends in Plant Science*, **13**, 631–639.
- Herlinawati, E., Montoro, P., Ismawanto, S., Syaafaah, A., Aji, M., Giner, M. *et al.*** (2022) Dynamic analysis of tapping panel dryness in *Hevea brasiliensis* reveals new insights on this physiological syndrome affecting latex production. *Heliyon*, **8**, e10920.
- Jacob, J.L.** (1989) Yield-limiting factors, latex physiological parameters, latex diagnosis and clonal typology. In: d'Auzac, J., Jacob, J.L. & Chrestin, H. (Eds.) *Physiology of rubber tree latex*. Boca Raton, FL: C.R.C. Press, pp. 345–381.
- Junaidi, J., Nuringtyas, T.R., Clément-Vida, I.A., Flori, A., Syaafaah, A., Oktavia, F. *et al.*** (2022) Analysis of reduced and oxidized antioxidants in *Hevea brasiliensis* latex reveals new insights into the regulation of antioxidants in response to harvesting stress and tapping panel dryness. *Heliyon*, **8**, e09840.
- Leclercq, J., Wu, S.Y., Farinas, B., Pointet, S. & Montoro, P.** (2020) Post-transcriptional regulation of several biological processes involved in latex production in *Hevea brasiliensis*. *PeerJ*, **8**, e8932.
- Li, D.J., Deng, Z., Chen, C.L., Xia, Z.H., Wu, M., He, P. *et al.*** (2010) Identification and characterization of genes associated with tapping panel dryness from *Hevea brasiliensis* latex using suppression subtractive hybridization. *BMC Plant Biology*, **10**, 140.

- Li, D.J., Wang, X.C., Deng, Z., Liu, H., Yang, H. & He, G.M. (2016) Transcriptome analysis reveal molecular mechanism underlying tapping panel dryness of rubber tree (*Hevea brasiliensis*). *Scientific Reports*, **6** (23), 540.
- Li, D.J., Wu, S.H. & Dai, L.J. (2020) Current progress in transcriptomics and proteomics of latex physiology and metabolism in the *Hevea brasiliensis* rubber tree. In: Matsui, M. & Chow, K.S. (Eds.) *The rubber tree genome*. Springer Nature: Switzerland AG, pp. 127–129.
- Liu, H., Wei, Y.X., Deng, Z., Yang, H., Dai, L.J. & Li, D.J. (2019) Involved of HbMC1-mediated cell death in tapping panel dryness of rubber tree (*Hevea brasiliensis*). *Tree Physiology*, **39**, 391–103.
- Liu, J.P., Xia, Z.Q., Tian, X.Y. & Li, Y.J. (2015) Transcriptome sequencing and analysis of rubber tree (*Hevea brasiliensis* muell.) to discover putative genes associated with tapping panel dryness (TPD). *BMC Genomics*, **16**, 398.
- Men, X., Wang, F., Chen, G.Q., Zhang, H.B. & Xiao, M. (2019) Biosynthesis of natural rubber: current state and perspectives. *International Journal of Molecular Sciences*, **20**, 50.
- Nie, Z.Y., Kang, G.J., Duan, C.F., Li, Y., Dai, L.J. & Zeng, R.Z. (2016) Profiling ethylene-responsive genes expressed in the latex of the mature virgin rubber trees using cDNA microarray. *PLoS One*, **11**, e0152039.
- Nie, Z.Y., Kang, G.J., Li, Y., Dai, L.J. & Zeng, R.Z. (2015) Whole-transcriptome survey of the putative ATP-binding cassette (ABC) transporter family genes in the latex-producing laticifers of *Hevea brasiliensis*. *PLoS One*, **10**, e0116857.
- Nie, Z.Y., Wang, Y.H., Wu, C.T., Li, Y. & Zeng, R.Z. (2018) Expression patterns of the acyl-CoA-binding protein family members in laticifers are possibly involved in lipid and latex metabolism of *Hevea brasiliensis* (the Para rubber tree). *BMC Genomics*, **19**, 5.
- Niephaus, E., Muller, B., van Deenen, N., Lassowdkat, I., Monin, M., Finke-meier, I. et al. (2019) Uncovering mechanisms of rubber biosynthesis in *Taraxacum koksaghyz*-role of cis-prenyltransferase-like 1 protein. *The Plant Journal*, **100**, 591–609.
- Pandey, A. & Mann, M. (2000) Proteomics to study genes and genomes. *Nature*, **405**, 837–846.
- Peng, S.Q., Wu, K.X., Huang, G.X. & Chen, S.C. (2011) HbMyb1, a Myb transcription factor from *Hevea brasiliensis*, suppresses stress induced cell death in transgenic tobacco. *Plant Physiology and Biochemistry*, **491**, 429–1435.
- Putranto, R.A., Herlinawati, E., Rio, M., Leclercq, J., Piyatrakul, P., Gohet, E. et al. (2015) Involvement of ethylene in the latex metabolism and tapping panel dryness of *Hevea brasiliensis*. *International Journal of Molecular Sciences*, **16**, 17885–17908.
- Putranto, R.A. & Montoro, P. (2016) The *Hevea brasiliensis* AP2/ERF superfamily: from ethylene signalling to latex harvesting and physiological disease response. *Menara Perkebunan*, **84**, 49–62.
- Rojruthai, P., Sakdapipanich, J.T., Takahashi, S., Hyegin, L., Noike, M., Koyama, T. et al. (2010) *In vitro* synthesis of high molecular weight rubber by *Hevea* small rubber particles. *Journal of Bioscience and Bioengineering*, **109**, 107–114.
- Sando, T., Takeno, S., Watanabe, N., Okumoto, H., Kuzuyama, T., Yamashita, A. et al. (2008) Cloning and characterization of the 2-C-methyl-D-erythritol 4-phosphate (MEP) pathway genes of a natural-rubber producing plant, *Hevea brasiliensis*. *Bioscience Biotechnology & Biochemistry*, **72**, 2903–2917.
- Scott, D.J., da Costa, B.M., Espy, S.C., Keasling, J.D. & Cornish, K. (2003) Activation and inhibition of rubber transferases by metal cofactors and pyrophosphate substrates. *Phytochemistry*, **64**, 123–134.
- Siler, D.J. & Cornish, K. (1993) A protein from *Ficus elastica* rubber particles is related to proteins from *Hevea brasiliensis* and *Parthenium argentatum*. *Phytochemistry*, **32**, 1097–1102.
- Sookmark, U., Pujade-Renaud, V., Chrestin, H., Lacote, R., Naiyanetr, C., Seguin, M. et al. (2002) Characterization of polypeptides accumulated in the latex cytosol of rubber trees affected by the tapping panel dryness syndrome. *Plant & Cell Physiology*, **43**, 1323–1333.
- Tanaka, Y., Aik-Hw, E.E., Ohya, N., Nishiyama, N., Tangpakdee, J., Kawahara, S. et al. (1996) Initiation of rubber biosynthesis in *Hevea brasiliensis*: characterization of initiating species by structural analysis. *Phytochemistry*, **41**, 1501–1505.
- Tang, C.R., Yang, M., Fang, Y.J., Luo, Y.F., Gao, S.H., Xiao, X.H. et al. (2016) The rubber tree genome reveals new insights into rubber production and species adaptation. *Nature Plants*, **2**, 1–10.
- Tausky, H.H. & Shorr, E. (1953) A micro colorimetric methods for the determination of inorganic phosphorus. *Journal of Biological Chemistry*, **202**, 675–685.
- Tristama, R., Mawaddah, P.A.S., Ade-fipriani, L. & Junaidi, J. (2019) Physiological status of high and low metabolism *Hevea* clones in the difference stage of tapping panel dryness. *Biodiversitas*, **20**, 267–273.
- Venkatachalam, P., Thulaseedharan, A. & Raghobama, K.G. (2009) Molecular identification and characterization of a gene associated with the onset of tapping panel dryness (TPD) syndrome in rubber tree (*Hevea brasiliensis* Muell.) by mRNA differential display. *Molecular Biotechnology*, **41**, 42–52.
- Wang, Y., Zhan, D.F., Li, H.L., Guo, D., Zhu, J.H. & Peng, S.Q. (2017) Transcriptome-wide identification and characterization of MYB transcription factor genes in the laticifer cells of *Hevea brasiliensis*. *Frontiers in Plant Science*, **8**, 1974.
- Wu, J.L. & Hao, B.Z. (1990) Ultrastructural observation of differentiation laticiferous in *Hevea brasiliensis*. *Journal of Integrative Plant Biology*, **5**, 350–354 + 415–416.
- Xie, W., McMahan, C.M., DeGraw, A.J., Distefano, M.D., Cornish, K. & Whalen, M.C. (2008) Initiation of rubber biosynthesis: *In vitro* comparisons of benzophenone-modified diphosphate analogues in three rubber-producing species. *Phytochemistry*, **69**, 2539–2545.
- Yamaguchi, T., Kurihara, Y., Makita, Y., Okubo-Kurihara, E., Kageyama, A., Osada, E. et al. (2020) Regulatory potential of bHLH-type transcription factors on the road to rubber biosynthesis in *Hevea brasiliensis*. *Plants (Basel)*, **9**, 674.
- Yamashita, S. & Takahashi, S. (2020) Molecular mechanisms of natural rubber biosynthesis. *Annual Review of Biochemistry*, **89**, 24.1–24.31.
- Yamashita, S., Yamaguchi, H., Waki, T., Aoki, Y., Mizuno, M., Yanbe, F. et al. (2016) Identification and reconstitution of the rubber biosynthetic machinery on rubber particles from *Hevea brasiliensis*. *eLife*, **5**, e19022.
- Yang, S.Q. & Fan, S.W. (1995) Physiological response of PR107 to intensive tapping with stimulation at early exploitation stage. *Chinese Journal of Tropical Crops*, **16**, 17–28.
- Yuan, H., Xu, Y., Chen, Y.Z., Zhan, Y.Y., Wei, X.T., Li, L. et al. (2019) Metabolomics analysis reveals global acetoin stress response of *Bacillus licheniformis*. *Metabolomics*, **15**, 25.
- Zhang, Y., Leclercq, J. & Montoro, P. (2017) Reactive oxygen species in *Hevea brasiliensis* latex and relevance to tapping panel dryness. *Tree Physiology*, **37**, 261–269.
- Zhang, Y., Li, Z.X., Yu, X.D., Fan, J., Pickett, J.A., Jones, H.D. et al. (2015) Molecular characterization of two isoforms of a farnesyl pyrophosphate synthase gene in wheat and their roles in sesquiterpene synthesis and inducible defence against aphid infestation. *New Phytologist*, **206**, 1101–1115.